JSR Publications

Available Online

J. Sci. Res. **15** (3), 831-843 (2023)

JOURNAL OF SCIENTIFIC RESEARCH

www.banglajol.info/index.php/JSR

Biogenic Synthesis, Characterization of Cerium Oxide Nano Particles using *Perioria pinnatum* Leaf Extract and Its Applications

R. Madhu[1], K. Pruthviraj[2], S. Sreenivasa[1,3], D. Suresh[2], B. E. K. Swamy[4], M. S. Prakash[1*]

[1]Department of Studies and Research in Chemistry, Tumkur University, Tumakuru-572 103, Karnataka, India

[2]Department of Studies and Research in Organic Chemistry, Tumkur University, Tumakuru-572 103, Karnataka, India

[3]Deputy Adviser, National Assessment and Accreditation Council, Nagarbhavi, Bengaluru-560 072, Karnataka, India

[4]Department of Industrial Chemistry, Kuvempu University, Shivamogga-577 203, Karnataka, India

Received 18 January 2023, accepted in final revised form 6 June 2023

Abstract

The biogenic method of synthesis of metal oxide nanoparticles is the recent advances development in nanotechnology, and cerium oxide (CeO_2) nanoparticles (NPs), in particular, are advantageous due to their remarkable properties. In this report, we discuss the results of Cerium oxide NPs synthesized by solution-combustion method using "*Perioria pinnatum"* leaf extract as a reducing and stabilizing agent. The structurally spherical shaped CeO_2 NPs with 12 nm crystal size were synthesized and further characterized by powder X-ray diffraction analysis (PXRD), Fourier transforms infrared spectroscopy (FT-IR), and Scanning electron microscopy (SEM) and with Energy dispersive X-ray (EDX) analysis. XRD pattern confirmed the formation of CeO_2 NPs with FCC structure. Further, green synthesized CeO_2 nanoparticles were assessed for their *in-vitro* antioxidant activity, visible light-induced dye degradation property against methylene blue, and in electrical cells modified with CeO_2 NPs that could electrochemically sense Dopamine (DA) up to 11 µM.

Keywords: CeO_2 NPs; Prioria pinnatum; PXRD; FT-IR; Dopamine sensing.

doi: http://doi.org/10.3329/jsr.v15i3.64001 J. Sci. Res. **15** (3), 831-843 (2023)

1. Introduction

Among the leading research fields, nanotechnology has gained remarkable interest in every field of science and technology because of its multitude of applications in the field of healthcare, electronics, imaging, and other numerous scientific disciplines, unique physicochemical properties of nanoscale structures (1-100 nm) will be utilized in various field of science [1-5]. Metal oxide nanomaterials can be prepared by many methods, such as hydrothermal, combustion synthesis, gas-phase methods, microwave synthesis, and sol-gel processing [6]. However, the above methods utilize toxic reagents, and notably, the

* *Corresponding author*: shirsatpm@gmail.com

NPs obtained were toxic, unstable, and less efficient. Thus, the less toxic approach known as green synthesis has been adopted by researchers using various eco-friendly resources such as plant and other biological derivatives [9-14]. The biosynthetic route of synthesis of nanoparticles offers a wide range of advantages since the biological extracts have rich sources of phytochemicals, which assist in the reduction and stabilization of nanoparticles [15-18]. Among the metal oxide nanoparticles, Cerium oxide nanoparticles (CeO_2 NPs) have been widely studied because of their unique structural, chemical, and physical properties [19,20]. CeO_2 can produce an oxygen vacancy in the lattice [21,22]; therefore, the redox properties of CeO_2 NPs are helpful for understanding various diseases associated with oxidative stress problems. CeO_2 NPs can also produce several reactive oxygen species (ROS) crucial for *in vitro* activities [23,24].

"Perioria pinnatum" is a vulnerable and endangered medicinal plant belonging to the family *Fabaceae.* In particular, the oleo-gum-resin is used in treating gonorrhea, catarrhal conditions of Genito-urinary as well as respiratory tracts [25], and also in curing sores of elephants. It is well-established that plant-derived compounds offer numerous sources of antioxidant, antidiabetic and antiobesity, and antimicrobial agents. The scientific and pharmacological formulation of *"Perioria pinnatum"* has not been established through tribes of the region are traditionally using it. An ethnobotanical search reveals the use of many traditional herbs in the treatment of various diseases, which are usually free from side effects, are economical and also accessible to humans, and provide significant potential for the development of novel biomolecules [26-28]. Currently, plant-mediated synthesis of metallic nanoparticles is gaining importance, and there are no reports on the synthesis of CeO_2 NPs using *"Perioria pinnatum*". In this study, CeO_2 NPs were prepared using "*Perioria pinnatum"* leaf extract. They evaluated its in-vitro antioxidant activity and visible light-induced dye degradation property against methylene blue, and cells modified with CeO_2 NPs could electrochemically sense Dopamine.

Based on the above multifunctional applications of biogenic CeO_2 NPs, the present study focuses on the synthesis of CeO_2 NPs through an eco-friendly combustion route using different concentrations of "*Perioria pinnatum"* leaf extract as fuel. The formed nanoparticles are characterized by PXRD, SEM, UV-Visible absorption, and FT-IR techniques. Further, the CeO_2 NPs are evaluated for their photocatalytic and biological applications, like antioxidant and antibacterial properties.

2. Materials and Methods

Chemicals that are used in this work were of analytical grade and used as received without further purification. Ceric ammonium nitrate $[NH_4]_2[Ce(NO_3)_6]$ methanol (CH_3OH), 2,2-diphenyl-1-picrylhydrazyl (DPPH), acetic acid (CH_3COOH) and sodium hydroxide (NaOH) were purchased from Sigma Aldrich and "*Perioria pinnatum"* leaves extract.

2.1. *Collection of "Perioria pinnatum" leaf and preparation of leaf extract*

Leaves of the "*Perioria pinnatum"* plant were collected from the Namada Chilume medical plant park, Tumakuru district. Tumakuru Karnataka. The collected leaves were washed with distilled water several times to remove the dust particles and other impurities, then dried for 20 days to remove the moisture. These dried leaves were powdered roughly and stored in an airtight bottle for further use. Then 50 g of powdered "*Perioria pinnatum* " leaves were refluxed with water for about 5hr, and the extracted solution was cooled to room temperature and filtered using a Whatman No.1 filter paper. The extract was concentrated and stored in the refrigerator for further use.

2.1.1. *Green Synthesis of CeO_2 nanoparticles*

2 g of concentrated plant extract was dissolved in a 100 mL standard flask using distilled water and previously weighed 5.48 gm of ceric ammonium nitrate $[NH_4]_2[Ce(NO_3)_6]$ was added to 25 mL of this plant extract solution and heated hot plate at a high temperature about 400-500 °C, the reaction was completed within 5 to 6 minutes finally to get light yellow colored CeO_2 NPs. Then it was allowed to cool to room temperature. Further, the obtained precipitates were calcinated for 4 h at 400 °C to evaporate and powdered by mortar and pestle to get a fine powder. The same experiment was repeated with 30 and 35 mL of plant extract (Table 1).

Table 1. CeO_2 NPs prepared with different volumes of fuel.

Sample code	$CeH_{12}N_3O_{15}$ (g)	Plant extract (mL)
M1	5.48	25
M2	5.48	30
M3	5.48	35

2.2. *Characterization techniques*

The X-ray diffraction of CeO_2 NPs was performed on Shimadzu 7000 diffractometer using CuKα radiation (λ=1.54 nm). Morphology was observed by employing Hitachi Table Top Microscope Model TM 3000. UV-Vis spectra of synthesized CeO_2-NPs were recorded in water after sonication for 10 min using Shimadzu UV-1800 UV-Visible spectrophotometer. CeO_2 NPs were also chareacterized by Fourier transform infrared spectroscopy (FTIR, Thermo Fischer Scientific, Waltham, MA, USA). A cyclic voltammetry study was performed using a single-compartment, three-electrode cell with MCPEs prepared with nanoparticles as the working electrode. An aqueous saturated calomel electrode (SCE) was used as the reference electrode, and a Pt wire was the auxiliary electrode. All potentials were measured and reported vs. the SCE. The cyclic voltammetry (CV) measurements were performed on a model 660c (CH Instruments) potentiostat/galvanostat.

2.3. *Antioxidant activity: DPPH radical scavenging assay*

The stock solution was prepared by dissolving 20, 40, 60, 80, and 100 mg of CeO_2 NPs in 10 mL of de-ionized water. Various concentrations of CeO_2 NPs (20, 40, 60, 80, and 100 µL) were added to 50 % aqueous methanol and 145 µL of 2, 2-diphenyl-1-picrylhydrazyl (DPPH) and incubated in darkness at 37 °C for 30 min. Absorbance was measured at 520 nm against 50 % methanol as blank and ascorbic acid was used as the standard. A control reaction was carried out without the addition of the test sample. The antioxidant activity of Green synthesized CeO_2 NPs was evaluated using the following formula [29].

$$\% \text{ Inhibition} = \frac{\text{Absorbance of control} - \text{Absorbance of sample}}{\text{Absorbance of control}} \times 100$$

2.4. *Photocatalytic dye degradation*

The photocatalytic activity of CeO_2 NPs was studied using methylene blue (MB) aqueous solution (5 ppm). During the color removal test, 20 mg of ceria NPs were added to 100 mL of dye solution. The absorbance of standard dye was recorded, and the whole setup was kept under sunlight with constant stirring. About 2 mL of suspension was withdrawn at each 20 min interval of time, and the absorbance was recorded at 665 nm using a UV-visible spectrophotometer. The photodegradation efficiency of methylene blue was calculated using the following equation.

$$\% \text{ of degradation} = \frac{C_i - C_f}{C_i} \times 100$$

Where C_i = Initial concentration of MB, C_f = Final concentration of MB in the solution after irradiation for a given time interval.

2.5. *Modified electrode preparation and sensing*

The bare carbon paste electrode (bare CPE) was prepared by mixing 80 % graphite powder with 20 % silicon oil in an agate mortar for approximately 30 min to produce a homogenous carbon paste. The paste was packed into the homemade cavity and smoothed on a piece of weighing paper. The modified carbon-paste electrode (MCPE) was prepared by adding 4 mg of CeO_2 NPs to the previously prepared graphite powder/silicon oil mixture.

3. Results and Discussion

3.1. *X-ray Diffraction analysis (XRD)*

CeO_2 NPs synthesized at different concentrations, such as 25, 30, and 35 mL of "*Perioria pinnatum"* leaf extract, show diffraction patterns shown in Fig 1. were well indexed to that of standard diffraction data. The diffraction peaks positioned at 28, 34, 48, 58, and 76,

corresponding to the (111), (200), (220), (222), and (311) planes of CeO_2 correspond to the face-centered cubic system in accordance with cubic fluorite structure with space group Fm-3m (JCPDS card. No.81- 0792). For the calculation of average particle size Debye-Scherrer formula was used for the strong peaks at 28 (111), 34 (200), 48 (220), and 58 (222) were considered, and the crystallite sizes were found to be around 10-12 nm [30].

$$\text{Average crystalline size (D)} = \frac{0.9\lambda}{\beta\cos\theta}$$

Where λ = wavelength of the X-ray used for the analysis, β = angular peak width at half maxima (in radians), θ = Bragg's diffraction angle

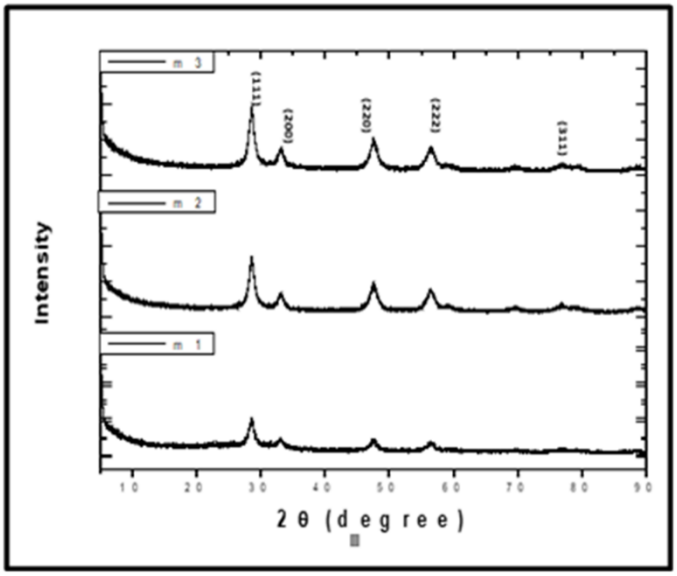

Fig. 1. PXRD of CeO_2 NPs obtained by the addition of 25, 30, and 35 mL of plant extract.

3.2. *FT-IR Spectroscopy*

The FT-IR spectra of CeO_2 NPs are shown in Fig. 2. The broad absorption band located around 3400 cm^{-1} corresponds to the O–H stretching vibration of residual water and hydroxyl groups, while the absorption band at 1630 cm^{-1} is due to the scissor bending mode of associated water. The band at 648 cm^{-1} corresponds to the metal-oxygen bond and N-O at 1400 cm^{-1} as per the literature [31,32].

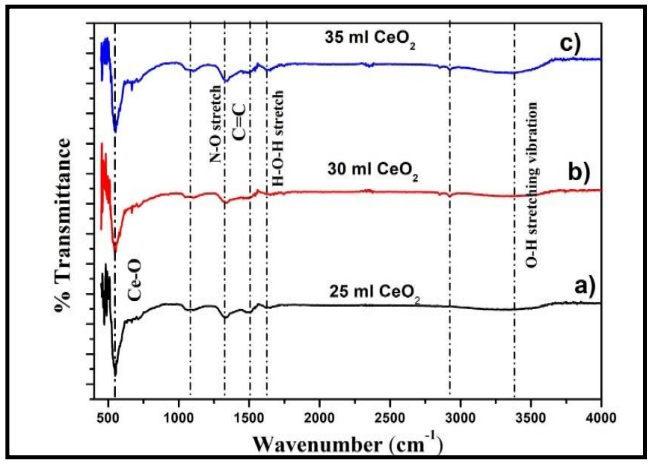

Fig. 2. Infrared spectra of CeO_2 NPs prepared with (a) 25, (b) 30, and (c) 35 mL of plant extracts.

3.4. UV-Vis and DRS analysis

The Green synthesized CeO_2 NPs UV-Vis spectrum is depicted in Fig. 3. The absorption maximum is around 350 nm at the UV region, which was related to the charge transfer transition from oxygen 2p to cerium 4f orbitals, indicating the formation of CeO_2 NPs.

In the Diffuse reflectance (DR) spectra of CeO_2 NPs, an absorption edge at around 350 nm was observed due to the electronic transitions from O 'P' orbitals to the Ce'd' orbitals, as shown in Fig. 4a. The Kubelka-Munk (KM) function, was utilized to estimate the energy band gap of the prepared samples. The graph of $[F(R)hv]^2$v/s energy (hv) was plotted, as shown in Fig. 4b. Band edge of CeO_2 NPs was estimated by extrapolating the curve $[F(R)hv]^2$ to zero. The band edges measured by extrapolation were found to be 3.08 eV. Generally, the deviation in the band edge or gap was related to certain factors, i.e., variation in crystallite size, lattice parameter, oxygen vacancies, etc. [33-35].

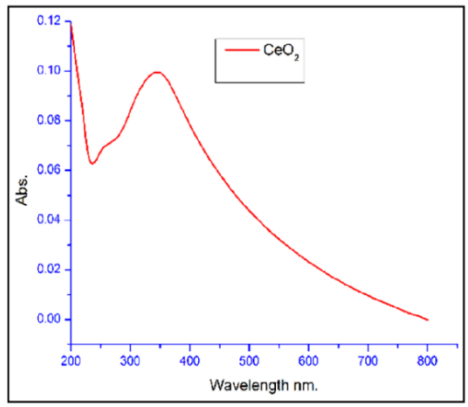

Fig. 3. UV-Vis spectrum of Green synthesized CeO_2 NPs.

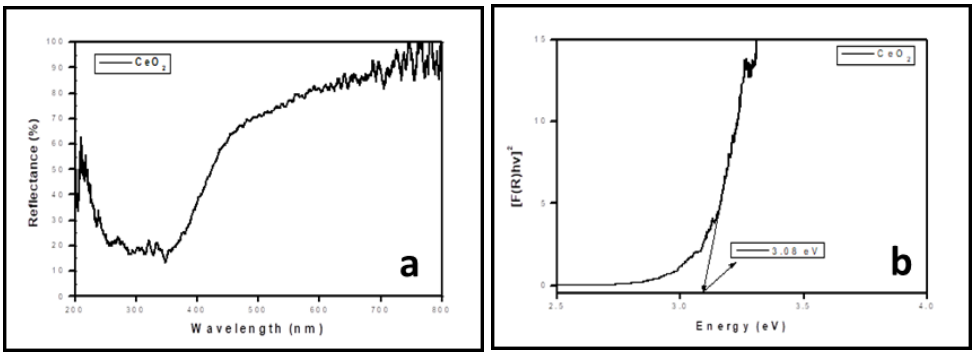

Fig. 4. a) DR spectra and b) energy bandgap of CeO_2 NPs.

3.5. *SEM and EDX analysis*

The SEM analysis of the synthesized CeO_2 NPs M1, M2 & M3 using "*Perioria pinnatum"* leaf extra was depicted in Fig. 5, M1(a), M2(b), M3(c) & EDX(d)) respectively. The morphological observation indicated that green synthesized CeO_2 NPs were homogenous with spherical nature. M1 and M2 showed agglomeration leading to affected morphology except for M3. Hence we further continued our studies with this sample. The elemental compositions of the prepared CeO_2 NPs were subjected to EDAX analysis and showed a unique set of peaks.

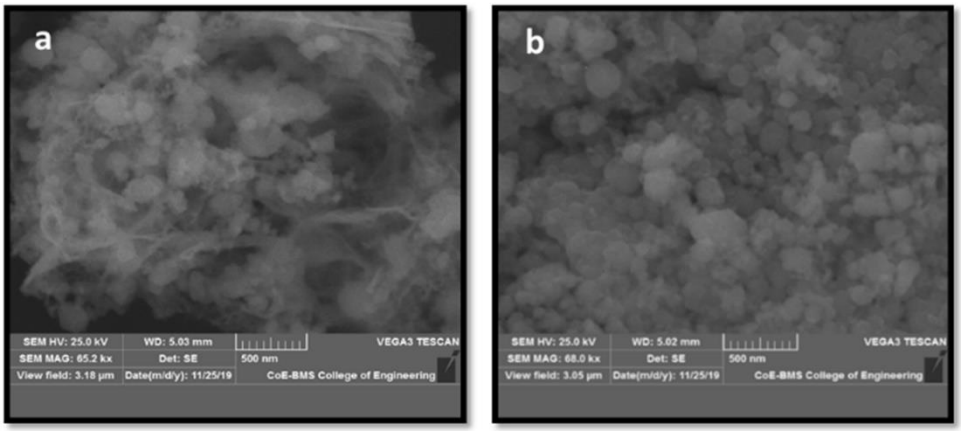

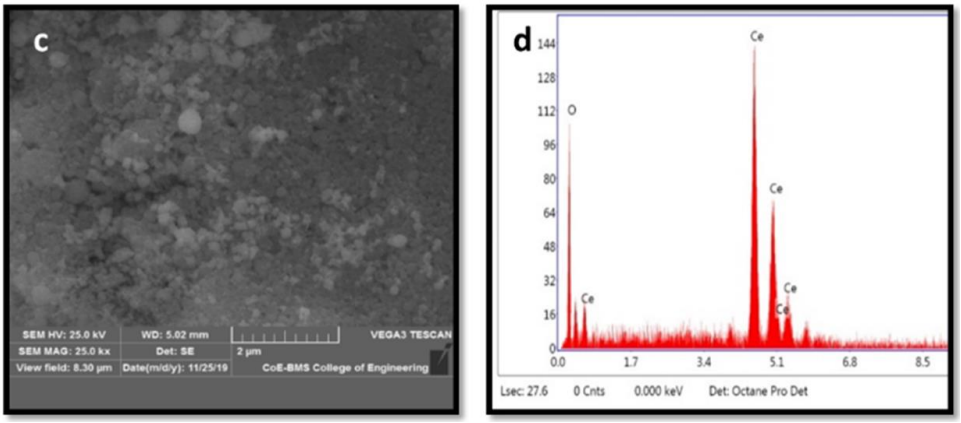

Fig. 5. SEM images of CeO_2 NPs obtained by the addition of a) 25, b) 30, c) 35 mL of plant extracts and d) EDX analysis.

3.6. *Antioxidant activity*

The antioxidant activity can be analyzed by different methods, both *in vitro* and *in vivo*. Among *in vitro* assays, the DPPH•-based method is probably the most popular one due to its simplicity, speed, and low cost [36]. DPPH (1,1-diphenyl-2-picrylhydrazyl) is a stable free radical that can be reduced by transferring hydrogen from other compounds. On the other hand, assays allow an analysis under physiological conditions but require animal models; some of them (like mammals) are expensive and very time-consuming.

Antioxidant activity was carried out by the DPPH assay using a modified method of Brand- Williams. 1, 1-diphenyl-2-picrylhydrazyl is a stable free radical that produces purple color when dissolved in methanol. In the presence of antioxidants, the DPPH radical decays and becomes colorless or pale yellow, and the change in absorbance can be measured spectrophotometrically at 520 nm, the characteristic absorption wavelength of DPPH. The radical scavenging activity (RSA) values were expressed as the ratio percentage of sample absorbance decrease and the absorbance of DPPḢ solution in the absence of the test sample at 520 nm. The antioxidant potency of CeO_2 was shown graphically in Fig. 6. The CeO_2 was proved to be potent at inhibiting the DPPH free radical scavenging activity with an IC_{50} value of 79.68 µg/mL; readings were tabulated in Table 2.

Table 2. DPPH free radical scavenging activity of CeO_2 NPs.

Test tube NO	Concentration (µg)	NPS sample (µL)	DPPH solution (µL)	Incubated for 30 min at 37 °C	Absorbance at 520 nm
1	00.00	00.00	145		1.082
2	20.00	20.00	145		0.344
3	40.00	40.00	145		0.403
4	60.00	60.00	145		0.482
5	80.00	80.00	145		0.558
6	100.00	100.00	145		0.402

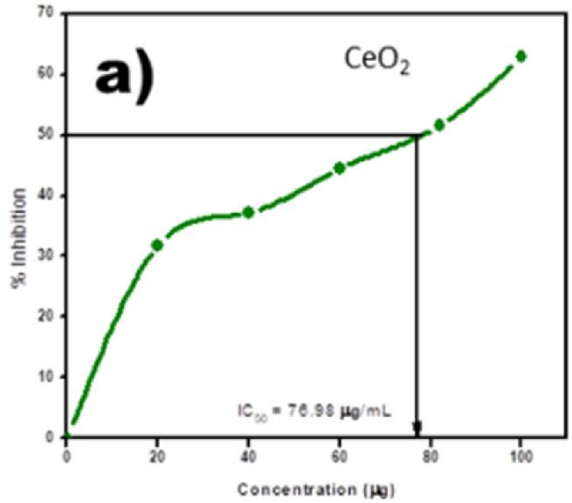

Fig. 6. The antioxidant potency of CeO_2.

1.3.6. *Visible light-induced photocatalytic dye degradation*

Nowadays, industries are responsible for dye effluents in the environment. Therefore, the textile industry generates more than half of dye effluents, with a worldwide dye discharge estimated at 280,000 tons/year [37]. Methylene blue (MB) is a common dye used as a dyeing agent in the textile industry. They are anionic and cationic dyes, respectively. The photodegradation efficiency depends on forming hydroxyl radicals, the critical species in the degradation process. When the CeO_2 catalyst was exposed to sunlight, electrons were generated in the conduction band, and holes were created in the valence band. Some of these charge carriers spread to the crystal surface and react with the adsorbed water molecules, OH^- ions, and oxygen molecules.

The photocatalytic activity of CeO_2 NPs was studied using methylene blue (MB) aqueous solution (5 ppm). During the color removal test, 20 mg of ceria nanoparticles were added to 100 mL of dye solution. The absorbance of standard dye was recorded, and the whole setup was kept under sunlight with constant stirring. About 2 mL of suspension was withdrawn at each 20 min interval of time, and the absorbance was recorded at 665 nm using a UV-visible spectrophotometer. Fig. 7. a) to c) shows the UV-Visible absorption spectra of MB as a function of the catalytic reaction time. The solution turns colorless after 100 min, which specifies that the complete degradation of dye molecules by CeO_2 reveals a better catalytic activity for a given dye molecule. After 100 min of reaction, it is observed that by using prepared nanoparticles, the dye solution with a concentration of 20 mg can be degraded up to 68 % by using CeO_2 NPs. Similarly, 40 mg and 60 mg can be degraded up to 72 % and 76 %, respectively. We could see the comparing the catalyst load against the activity, indicating that as the amount of catalyst increases, the % of degradation gradually increases. It has been confirmed that the synthesized CeO_2 possesses better photocatalytic activity under sunlight, predominantly

due to its smaller size, oxygen vacancy, and efficient charge separation. The CeO_2 effectively photo-decomposes MB dye in an aqueous solution.

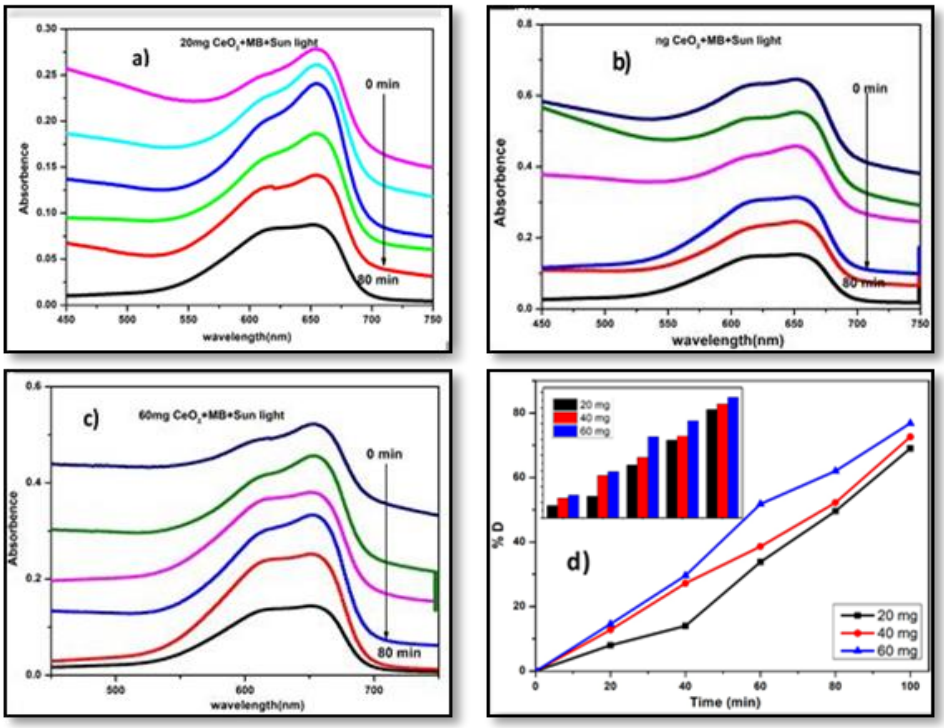

Fig. 7. Catalytic photodegradation of MB dye using a) 20, b) 40, and c) 60 mg of CeO_2 NPs catalyst and 'd' represents comparison.

3.7. *Electrochemical response of dopamine at CeO_2 NPs modified carbon paste electrode*

Cyclic voltammetry makes possible the elucidation of the kinetics of electrochemical reactions at the electrode surface. In a typical voltammogram, there can be several peaks. From the sweep-rate dependence of the possible to investigate the role of adsorption, diffusion, and coupled homogeneous chemical reaction mechanism. The selection and development of an active material is a challenge. The active sensing materials may be of any kind, whichever acts as a catalyst for sensing a particular analyte or a set of analytes. The recent development in nanotechnology has paved the way for many new materials and devices of desirable properties which have useful functions for numerous electrochemical sensor and biosensor applications [38-41].

The bare carbon-paste electrode (bare CPE) was prepared by mixing 80 % graphite powder with 20 % silicon oil in an agate mortar for approximately 30 min to produce a homogenous carbon paste. The paste was packed into the homemade cavity and smoothed on a piece of weighing paper. The modified carbon-paste electrode (MCPE) was prepared

by adding 4 mg of CeO_2 NPs. The Electrochemical detection of DA using carbon paste electrodes was studied using bare and modified carbon paste electrodes. Fig .8. Shows the CVs of $1X10^{-4}$M DA at bare and CeO_2 NPs modified CPE at scan rate 100mV/s. The electrochemical response of DA shows an increase in peak current at the CeO_2 nanoparticles modified CPE. CeO_2 NPs modified CPE pair of well-defined redox waves of DA was obtained with an increase in the redox peak currents (solid line). It was observed that the peak currents enhanced greatly at CeO_2 NPs-modified CPE, which provides a high surface area of the CeO_2 NPs, improved the electrode contacting area of DA, and it lowered the oxidation and reduction potential differences at NPs-modified carbon paste electrode [42,43].

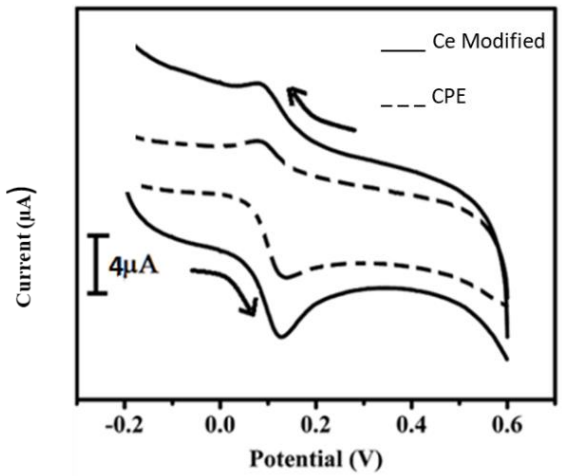

Fig. 8. Cyclic voltammogram of 1×10^{-4} M DA in PBS at pH 7.4 at the solid line for bare CPE and solid line for 4 mg CeO_2 NPs MCPE.

4. Conclusion

In the present work, CeO_2 NPs have been successfully synthesized by solution combustion method using "*Perioria pinnatum"* leaf extract because it is an easy, economical, non-toxic, and eco-friendly method. The synthesized CeO_2 NPs were subjected to a wide range of analytical techniques to confirm formation and morphology; further applications show good photodegradation and antioxidant activity exhibited by biogenic CeO_2 NPs compared with standards. Cyclic voltammetry studies proved the modified electrode with CeO_2 NPs has a good sensitizing ability toward detecting dopamine.

Acknowledgment

The authors are thankful to Tumkur University, Tumakuru, for providing the laboratory facility to carry out this work.

References

1. T. Kubik, K. Bogunia-Kubi, and M. Sugisaka, Curr. Pharm. Biotechnol. **6**, 1 (2005). https://doi.org/10.2174/1389201053167248
2. S. A. Nezhad, A. Es-haghi, and M. H. Tabriz, Appl. Organometal. Chem. **34**, ID e5314 (2019). https://doi.org/10.1002/aoc.5314
3. D. M. Smith, J. K. Simon, J. R. B. Jr, Nat. Rev. Immunol. **13**, 8 (2013). https://doi.org/10.1038/nri3488
4. H. E. Ahmed, Y. Iqbal, M. H. Aziz, M. Atif, *et al*., MDPI Molecules. **26**, 4659 (2021). https://doi.org/10.3390/molecules26154659
5. M. Nyoka, Y. E. Choonara, P. Kumar, P. P. D. Kondiah, and V. Pillay, MDPI Nanomater. **10**, 242 (2020). https://doi.org/10.3390/nano10020242
6. S. A. M. Ealias and M. P. Saravanakumar, Conf. Ser.: Mater. Sci. Eng. **263**, ID 032019 (2017). https://doi.org/10.1088/1757-899X/263/3/032019
7. S. Rajeshkumar and P. Naik, Biotechnol. Rep. **17**, 1 **(**2018). https://doi.org/10.1016/j.btre.2017.11.008
8. R. Magudieshwaran, J. Ishii, K. C. N. Raja, C. Terashima *et al*., Mater Lett. **239**, 40 (2019). https://doi.org/10.1016/j.matlet.2018.11.172
9. T. Arunachalam, M. Karpagasundaram, and N. Rajarathinam, Mater Sci. Poland **35**,791 (2017). https://doi.org/10.1515/msp-2017-0104
10. M. Darroudi, M. Sarani, R. K. Oskuee, A. K. Zak *et al*., Ceram. Int. **40**, 2041 (2014). https://doi.org/10.1016/j.ceramint.2013.07.116
11. K. M. Kumar, M. Mahendhiran, M. C. Diaz, N. H. Como, Mater Lett. **214**, 15 (2018). https://doi.org/10.1016/j.matlet.2017.11.097
12. Q. Maqbool, M. Nazar, S. Naz, T. Hussain *et al*., Int. J. Nanomed. **11**, 5015 (2016). https://doi.org/10.2147/IJN.S113508
13. P. Nithya, B. Murugesan, J. Sonamuthu, S. Samayanan, and S. Mahalingam, J. Photochem. Photobiol. B. **178**, 371 (2017). https://doi.org/10.1016/j.jphotobiol.2017.11.031
14. F. Charbgoo, M. B. Ahmad, and M. Darroudi, Int. J. Nanomed. **12**, 1401 (2017). http://dx.doi.org/10.2147/IJN.S124855
15. R. Pol and M. S. Yadawe, J. Emerg. Technol. Innovat. Res. **7**(3) (2020).
16. Á. G.Aponte, M. A. L. Ramírez, Y. C. Mora, J. F. S. Marín, and R. B. Sierra, AIMS Mater. Sci. **7**, 4 (2020). https://doi.org/10.3934/matersci.2020.4.468
17. A. Q. Khanjar, A. M. Farhan, and A. M. Rheima, J. Am. Inst. Chemist **94** (2023).
18. W. Yiling, G. K. Murakonda, and R. Jarubula, Mater. Res. Express **8**, 21 (2023). https://doi.org/10.1088/2053-1591/ac0fad
19. L. He, Y. Su, J. Lanhong, and S. Shi, J. Rare Earths **33**, 8 (2015). https://doi.org/10.1016/S1002-0721(14)60486-5
20. P. Duraisamy, Int. J. Res. Appl. Sci. Eng. Technol. **6**, 1 (2018). https://doi.org/10.22214/IJRASET.2018.1063
21. K. Anandalakshmi, P. Venkatachalam, and J. Venugobal, J. Sci. Res. **15**, 1 (2023). http://dx.doi.org/10.3329/jsr.v15i1.56206
22. M. ShafiqulIslam, M. T. Hossain, and A. Hannan. J. Bangladesh Acad. Sci. **46**, 2 (2022). http://dx.doi.org/10.3329/jbas.v46i2.60172
23. D. Taherzadeh, H. Amiri, S. Ebrahimi, A. Ghafarpour *et al*., Res. Square (2023). https://doi.org/10.21203/rs.3.rs-2568195/v1
24. P. Krishnaveni, M. L. Priya, and G. Annadurai, Life Science Informatics Publications **5**, 3 (2019). https://doi.org/10.26479/2019.0503.52
25. B. Subbaiyan, P. Samydurai, M. Karthik Prabu, R. Ramakrishnan, and V. Thangapandian, Our Nature **12**, 37 (2014). https://doi.org/10.3126/on.v12i1.12255
26. J. K. Kumar, A. G. D. Prasad, and S. A. Richard, Asian J. Plant Sci. Res. **1**, 4 (2011).
27. S. Sutha, V. R. Mohan, S. Kumaresan, C. Murugan, and T. Athiperumalsam, Ind. J. Traditional Knowledge **9**, 3 (2010).

28. A. P. Shahid, J. Traditional Complement. Medi. **7**, 380 (2017). https://doi.org/10.1016/j.jtcme.2016.12.003
29. M. Saravanan, S. Vigneshwar, G. B. Jegadeesan, and V. Ponnusami. Res. Square (2022). https://doi.org/10.21203/rs.3.rs-870597/v2
30. A. Arumugam, C. Karthikeyan, A. S. H. Hameed, K. Gopinath et al., Mater Sci. Eng. C: Biol. Appl. **49**, 2015. https://doi.org/10.2147/IJN.S113508
31. F. Abbas, J. Iqbal, T. Jan, M. S. H. Naqvi et al., J. Alloys Compd. **648**, 1060 (2015). https://doi.org/10.1016/j.jallcom.2015.06.195
32. J. Malleshappa, H. Nagabhushana, S. C. Sharma, Y. S. Vidya, *et al*., Spectrochim. Acta Part A: Molecular and Biomolecular Spectroscopy, **149**, 452 (2015). https://doi.org/10.1016/j.sintl.2020.100076
33. M. Darroudi, M. Hakimi, M. Sarani, R. K. Oskuee et al., Ceram. Int. **39**, (2013). https://doi.org/10.1016/j.ceramint.2018.07.201
34. E. K. Goharshadi, S. Samiee, and P. Nancarrow, J. Colloid Interface Sci. **356**, 473 (2011). https://doi.org/10.1016/j.jcis.2011.01.063
35. M. Gangwar, A. Dalai, A. Chaudhary, T. D. Singh, *et al*., Int. J. Pharm. Pharmaceutical Sci. **4**, 1 (2012).
36. X. Wang, J. Jiang, and W. Gao, Water Sci. Technol. **85**, 2076 (2022). https://doi.org/10.2166/wst.2022.088
37. C. Xia, W. Ning, W. Long, and G. Lin, Sens. Actuat. B. **147**, 629 (2010). https://doi.org/10.1007/s00216-012-6578-2
38. P. M. Ndangili, O. A. Arotiba, P. G. L. Baker, and E. I. Iwuoha, J. Electroanal. Chem. **643**, 77 (2010). https://doi.org/10.1016/j.jelechem.2010.03.006
39. K. Chetankumar, B. E. K. Swamy, and S. C. Sharma, Mater. Chem. Phys. **252**, ID 123231 (2020). https://doi.org/10.1016/j.matchemphys.2020.123231
40. N. B. Ashoka, B. E. K. Swamy, H. Jayadevappa, and S. C. Sharma. J. Electroanal. Chem. 85915 (2020).
41. M. Kumar, B. E. K. Swamy, C. Sravanthi, M. P. Kumar, and G. K. Jayaprakash, Mater. Chem. Phys. **284**, ID 126087 (2022). https://doi.org/10.1016/j.matchemphys.2022.126087
42. M. Shruthi Vishwanath, B. E. K. Swamy, and K. A. Vishnumurthy, Mater. Chem. Phys. **289**, ID 126443 (2022). https://doi.org/10.1016/j.matchemphys.2022.126443
43. K. Chetankumar, B. E. K. Swamy, and T. S. S. K. Naik, J. Mater. Sci.: Mater. Electron. **31**, 19728 (2020). https://doi.org/10.1007/s10854-020-04498-x